

Published in final edited form as:

Biochim Biophys Acta. 2013 May ; 1833(5): 1222–1234. doi:10.1016/j.bbamcr.2013.01.007.

Suppression of Androgen Receptor Enhances the Self-Renewal of Mesenchymal Stem Cells Through Elevated Expression of EGFR

Chiung-Kuei Huang¹, Meng-Yin Tsai², Jie Luo¹, Hong-Yo Kang², Soo Ok Lee^{1,*}, and Chawnschang Chang^{1,3,*}

¹George Whipple Lab for Cancer Research, Department of Pathology, Urology, and Radiation Oncology and the Cancer Center, University of Rochester Medical Center, Rochester, NY, USA

²Graduate Institute of Clinical Medical Sciences, Chang Gung University and Hospital, Kaohsiung, Taiwan

³Sex Hormone Research Center, China Medical University and Hospital, Taichung, Taiwan

Abstract

Bone marrow derived mesenchymal stem cells (BM-MSCs) have been widely applied in several clinical trials of diseases, such as myocardial infarction, liver cirrhosis, neurodegenerative disease, and osteogenesis imperfecta. Although most studies demonstrated that transplantation of BM-MSCs did exert a temporary relief and short-term therapeutic effects, eventually all symptoms recur, therefore it is essential to improve the therapeutic efficacy of transplantation by either elevating the self-renewal of BM-MSCs or enhancing their survival rate. Herein we demonstrated that the BM-MSCs and adipocyte derived mesenchymal stem cells (ADSCs) isolated from the androgen receptor (AR) knockout mice have higher self-renewal ability than those obtained from the wild-type mice. Knockdown of AR in MSC cell lines exhibited similar results. Mechanistic dissection studies showed that the depletion of AR resulted in activation of Erk and Akt signaling pathways through epidermal growth factor receptor (EGFR) activation or pathway to mediate higher self-renewal of BM-MSCs. Targeting AR signals using ASC-J9[®] (an AR degradation enhancer), hydroxyflutamide (antagonist of AR), and AR-siRNA all led to enhanced self-renewal of MSCs, suggesting the future possibility of using these anti-AR agents in therapeutic approaches.

Keywords

Epidermal growth factor receptor; Mesenchymal stem cells; Self-renewal; Androgen receptor; Androgen Receptor Knockout

Introduction

Bone marrow derived mesenchymal stem cells (BM-MSCs) are heterogeneous, pluripotent, and able to differentiate into multi-lineage mesodermal cell types, including osteocytes,

© 2012 Elsevier B.V. All rights reserved.

*Corresponding Authors: Soo Ok Lee (soook_lee@urmc.rochester.edu) and Chawnschang Chang (chang@urmc.rochester.edu).

Publisher's Disclaimer: This is a PDF file of an unedited manuscript that has been accepted for publication. As a service to our customers we are providing this early version of the manuscript. The manuscript will undergo copyediting, typesetting, and review of the resulting proof before it is published in its final citable form. Please note that during the production process errors may be discovered which could affect the content, and all legal disclaimers that apply to the journal pertain.

adipocytes, chondrocytes, and muscular cells. These pluripotent stem cells are thought to act as a reservoir for tissue regeneration after a normal cellular turnover or in some damaged tissues. Due to this characteristic of BM-MSCs, they have been widely applied in several clinical trials to treat diseases, such as myocardial infarction, liver cirrhosis, sepsis, and osteogenesis imperfecta [1–6]. Although scientists have shown exciting improvement effects at the beginning of the BM-MSC transplantation, eventually the symptoms recur [7]. Also, it has been shown that only low numbers of BM-MSCs can finally migrate to the damaged organs because microischemia causes the apoptosis of BM-MSCs during translocation [8]. Therefore, to improve the self-renewal and cell survival of BM-MSCs after transplantation is urgent and essential for the successful application of BM-MSCs in clinical use.

The antagonist of androgen, nilutamide has been reported to increase the proliferation of embryonic stem cells (ESCs) (Chang et al. 2006), indicating that androgen/androgen receptor (AR) might suppress the self-renewal of stem cells. However, the effects of androgens and AR on self-renewal of BM-MSCs have not been tested comprehensively. In addition, the gender differences in the function of activated BM-MSCs have also been suggested. Activated BM-MSCs are mainly responsible for the reactions to stress challenges including hypoxia and oxidative stress. Female BM-MSCs secrete more cytokines against stress challenges than male BM-MSCs [9, 10]. To utilize BM-MSCs transplantation in treating diseases, it is important to clarify how AR regulates functions of BM-MSCs. We therefore investigated AR effects on the self-renewal, proliferation, and differentiation of the BM-MSCs. The self-renewal of BM-MSCs is regulated by cellular intrinsic and extrinsic signaling. Extrinsic factors including fibroblast growth factor (FGF), insulin-like growth factor (IGF), epidermal growth factor (EGF), hepatocyte growth factor (HGF), and vascular endothelial growth factor (VEGF) all have been shown to affect stem cell behaviors [11–13]. The effects of HGF and VEGF have been tested in the transplantation of BM-MSCs for the preclinical myocardial infarction mouse model and the overexpression of HGF and VEGF significantly enhanced the recovery of myocardial infarction [14], suggesting that growth factors induced better self-renewal of mesenchymal stem cells allowing better therapy *in vivo*. Other cellular intrinsic signals, such as p-Erk1/2, phosphorylated signal transducer and activator of transcription 3 (p-STAT3), and p-Akt, have also been linked to the self-renewal, proliferation, and differentiation in different kinds of stem cells [14–18]. However, there have been no reports discussing how AR influences those signaling pathways to affect the self-renewal of BM-MSCs.

In this study, we isolated BM-MSCs and adipocyte derived mesenchymal stem cells (ADSCs) from the AR knockout (ARKO) male mice and wild type (WT) male littermates [19], and clearly demonstrated that depletion of AR enhanced the self-renewal of BM-MSCs and ADSCs. The enhanced self-renewal was shown by colony forming unit fibroblast (CFU-*f*) assays and other proliferation indices, because the CFU-*f* assay could be used to quantify the self-renewal potential of BM-MSC [20, 21]. During our mechanism studies, we identified that AR plays a negative role in the self-renewal of BM-MSCs through suppression of Erk1/2 and Akt signaling via modulation of EGFR molecule. Finally, we demonstrated that the currently available compounds, ASC-J9[®] (an AR degradation enhancer) [22–24], AR-siRNA [25], and hydroxyflutamide (HF) all could promote self-renewal of the WT BM-MSCs, suggesting that depletion of AR in BM-MSCs can enhance self-renewal of BM-MSCs.

Results

BM-MSCs and ADSCs express AR

Primary ADSCs and BM-MSCs were isolated from 8 weeks old male mice. As shown in supplemental Table 1, the flow cytometric analysis results confirmed their identity by

exhibiting marker profiles consistent with the previous studies [11, 26]. The multi-lineage differentiation capacities were also characterized in the isolated ADSCs and BM-MSCs. The results exhibited that ADSCs were able to differentiate into osteoblasts and adipocytes (identified by Alizarin Red and Oil Red O staining, respectively in Figure 1A). The adipogenesis markers, aP2 (adipocyte fatty acid binding protein 4), LPL (lipoprotein lipase), and PPAR γ (Peroxisome proliferator-activated receptor gamma), were increased in differentiated ADSCs upon adipogenesis induction when compared with vehicle control (Figure 1C). The osteogenesis markers, BSP (bone Sialoprotein), Col1 (collagen 1), and OPN (Osteopontin), were elevated in the differentiated osteoblasts derived from ADSCs when induced with osteogenic media (Figure 1D). Similarly, the BM-MSCs also showed multi-lineage differentiation capabilities (Figure 1E, G, and H). When we investigated AR levels in BM-MSCs and ADSCs, we found low levels of AR expressions (Figures 1B and F).

Depletion of AR enhances self-renewal of BM-MSCs and ADSCs

In order to investigate whether AR affects self-renewal of BM-MSCs and ADSCs, we exploited the ARKO transgenic mice for studies. The BM-MSCs and ADSCs were isolated from the ARKO male mice and their wild type (WT) male littermates. To confirm whether AR is functional in WT MSCs, the MMTV luciferase assay was performed. We found AR in WT MSCs showed 2.5 times higher transactivation ability in transcribing MMTV luciferase when compared with the basal levels in ARKO MSCs (supplemental Figure 1). After validating that WT MSCs AR is functional, the CFU-*f* assay [20, 21] was performed to test their self-renewal ability. The BM-MSCs and the ADSCs isolated from the ARKO male mice exhibited higher CFU-*f* numbers than those of WT male littermates (Figure 2A and B), suggesting higher self-renewal in ARKO MSCs (AR expressions in BM-MSCs and ADSCs were shown in Figures 2A and 2B, respectively to demonstrate AR knockout efficiency.) Similar results were observed in sub-cultured BM-MSCs (P0 – 1 passage and P2- 3 passages, Figure 2C and D), indicating that the increased self-renewal of MSCs is not a transient phenomenon that only occurred in freshly prepared MSCs.

To confirm the differentiation ability of WT and ARKO BM-MSCs, osteogenic and adipogenic media were used to induce the BM-MSCs differentiation into adipocytes and osteoblasts, respectively. The results showed that the initiation timings of calcium deposition were around 21 days in both WT and ARKO MSCs and DMP1 expressions were robustly increased in WT and ARKO MSCs at day 21 (supplemental Figure 2), implying that AR did not influence the initiation timing of the osteocyte formation process (Figure 2E). This result suggests that higher numbers of CFU-osteoblast (CFU-O) and CFU-alkaline phosphatase (CFU-ALP) observed in ARKO BM-MSCs were due to the differential self-renewal potential between WT and ARKO BM-MSCs, but not the altered differentiation process (supplemental Figure 3A and B). We also found higher CFU-adipocyte in ARKO MSCs than WT MSCs (supplemental Figure 3C). The flow cytometric analysis results also revealed that WT and ARKO MSCs were similar in the stem cell surface marker profiles, while the original total bone marrow mononuclear cells showed no difference between WT and ARKO male mice (data not shown).

The established MSC cell lines, C3H10T1/2 (embryo derived MSC line) and D1 (BM-MSC line), were used to confirm the above findings. The AR overexpressed and knocked down stable clones of C3H10T1/2 and D1 cells were selected based on Western blot and qRT-PCR data (Figure 3A and D). To evaluate whether AR can affect self-renewal of established cell lines, their self-renewal potentials were examined by MTT assay. Since all of them were stem cells, cell growth assay could be used to quantify their cell numbers to determine their self-renewal. The results showed that knockdown of AR in C3H10T1/2 cells promoted their

cell growth (Figure 3B), whereas overexpression of AR repressed their growth (Figure 3C). Similar results were observed in D1 stable clones (Figure 3E and F).

AR inhibits proliferation of BM-MSCs and ADSCs, but has little effect on apoptosis

Since the MTT assay is used to measure viable cells, we speculated that the growth inhibition results might be from the combined effects of proliferation and apoptosis differences. To answer whether depletion of AR promotes stem cell proliferation or inhibits stem cell apoptotic death, several proliferation/apoptosis assays were performed. We found ARKO BM-MSCs show higher positive Ki67 staining (Figure 4A) and BrdU labeling (Figure 4B) than WT BM-MSCs. Similar results were obtained in ADSCs showing higher numbers of Ki67 positive cells in ARKO ADSCs than in WT cells (Figure 4C). MTT assay results showed the promoted growth in AR knocked out ADSCs (Figure 4D). Higher expressions of proliferating cell nuclear antigen (PCNA) were detected in ARKO ADSCs than WT ADSCs (Figure 4E). In contrast, no significant difference in apoptotic death was observed between WT and ARKO BM-MSCs (Figure 4F and G), indicating that the depletion of AR caused elevated self-renewal in BM-MSCs and ADSCs and is due to proliferation effects rather than apoptotic death.

AR acts as a suppressor in the self-renewal potential of stem cells through inhibiting Akt and Erk1/2 signaling via EGFR

To dissect the potential mechanism by which targeting AR enhances self-renewal of BM-MSCs, p16 (Ink4a) and p19 (Arf) levels in ARKO and WT BM-MSCs were examined, since they were shown to play important roles in regulating stem cell self-renewal [27, 28]. We found that targeting AR either in primary BM-MSCs or in C3H10T1/2 (mouse mesenchymal stem cell lines) did not affect the expressions of p16 and p19 (Figure 5A-I). On the other hand, other key regulators, such as Erk1/2, Akt, and STAT3 were also reported to play important roles in maintaining the stemness and promoting the self-renewal of stem cells [14–18]. Our results showed that higher p-Akt and p-Erk1/2 levels, but not higher p-STAT3 expression, were observed in ARKO BM-MSCs and ADSCs as compared to WT controls (Figure 5J and K). Similar results were obtained in C3H10T1/2 and D1 cells (Figure 5L and M). The reporter assay of Elk1, one of the downstream signaling molecules of p-Erk1/2, was performed to validate Erk1/2 signaling transduction and the result showed that overexpression of AR in C3H10T1/2 suppressed the Elk1 transactivation (Figure 5N).

This signaling was further confirmed via blocking Erk1/2 and Akt pathways with the inhibitors, PD98059 (MEK1 inhibitor) and LY294002 (inhibitor of phosphatidylinositol 3 kinase). Blocking p-Erk1/2 and p-Akt with inhibitors completely reversed the ARKO enhanced self-renewal of BM-MSCs (Figure 5O and P). The PCNA expressions were determined to further validate the observation and we found that the treatments with p-Erk1/2 and p-Akt inhibitors partially masked the PCNA difference between WT and ARKO BM-MSCs (Figure 5Q). We therefore concluded that knockout of AR promotes the self-renewal potential of MSCs through activating Erk1/2 and Akt signaling.

EGFR, HGF, VEGF, FGFs, and IGF are upstream of Erk1/2 and Akt and reported to modulate the self-renewal of stem cells [12, 13, 29], and AR has been suggested to affect those molecules [30–33]. We therefore investigated the expressions of these molecules to determine which molecule is upstream of Erk1/2 and Akt signaling and critical in ARKO mediated self-renewal. The results revealed that the expressions of HGF, VEGF-B, and VEGF-C mRNAs were not significantly altered in WT and ARKO BM-MSCs (Figures 6A, B, and C). mRNA levels of HGF, VEGF-B, VEGF-C, FGF7, and FGF10 in CH3H10T1/2 cell line were found to be not significantly different after manipulating AR expression (Figure 6D-H). We then further tested AR effects on EGFR expression, since AR and EGFR

interaction has been demonstrated in prostate cancers [30, 31]. We found both short-term and long-term androgen treatments significantly promoted AR to translocate into the nucleus (supplemental Figure 4). In addition, as shown in Figure 6I and J, knockdown of AR in C3H10T1/2 and D1 cells increased the expressions of EGFR and p-EGFR, whereas overexpression of AR in C3H10T1/2 and D1 cells inhibited the expressions demonstrating that negative correlation of EGFR level and AR expression. Activation of Erk signaling along with pEGFR level was also negatively correlated with the AR level (Figure 6K). The ARKO BM-MSCs exhibited significantly higher expressions of EGFR mRNAs than WT BM-MSCs (Figure 6L). Overexpression of AR in C3H10T12 cells suppressed EGFR mRNA expression (Figure 6M).

To dissect the molecular mechanism by which AR regulates EGFR expression, we constructed the pGL3-luciferase vector containing EGFR promoter regions to test AR effects on EGFR transactivation. We found AR suppressed EGFR promoter activity in dose dependent manner, suggesting that AR mediated EGFR expression at the transcriptional level (Figure 6N and supplemental Figure 5). To see whether AR mediated EGFR expression is involved in ARKO enhanced self-renewal of BM-MSCs, we used EGFR inhibitor (AG1478) to treat ARKO BM-MSCs and found EGFR inhibitor treatment abolishes the ARKO enhanced self-renewal of BM-MSCs (Figure 6O). Conversely, administration of epidermal growth factor (EGF) in WT BM-MSCs increased CFU-*f* number and enhanced PCNA expressions (Figure 6P and Q), suggesting that EGF could promote the self-renewal of BM-MSCs even in the presence of AR, which suppresses EGFR expression. The p-EGFR and p-Erk1/2 were examined to see whether EGFR signaling was activated upon EGF addition and we found that addition of EGF activates EGFR and Erk1/2 signaling (Figure 6R). In summary, the antagonistic effects of AR on the self-renewal of BM-MSCs are considered to be through the EGFR, because activation of EGFR signaling with EGF still can overcome the AR effects in suppressing the self-renewal potential of BM-MSCs.

Taken together, the results from Figures 5 and 6 suggested that AR plays a suppressive role in the self-renewal of MSCs through suppression of the EGFR expression, which in turn, leads to inactivation of Akt and Erk signaling. The brief signaling cartoon is presented in Figure 7.

Treatments with anti-androgen/anti-AR drugs promote the self-renewal of BM-MSCs from WT mice but not from ARKO mice

The three currently available methods, HF, ASC-J9[®], and lentiviral siRNA, for targeting AR were then applied to determine if suppression of AR in BM-MSCs using these methods yields the similar effects as the results observed in the ARKO male mouse studies. Treatment with HF increased the self-renewal of WT BM-MSCs (Figure 8A), but not ARKO BM-MSCs (Figure 8B). The HF effect on the activation of EGFR signaling was examined by western blotting and the results exhibited that the expressions of p-EGFR, EGFR and p-Erk were enhanced upon HF treatment (Figure 8C and D). The similar effects were observed in the BM-MSCs treated with ASC-J9[®] (Figure 8C). The *in vitro* and *in vivo* effects of ASC-J9[®] on AR degradation have been reported previously [22–24]. Our CFU-*f* assay results showed that ASC-J9[®] enhanced the self-renewal of BM-MSCs in WT male mice (Figure 8E), but had no effects on ARKO BM-MSCs (Figure 8F). Furthermore, we examined the effect of infection with the lentivirus packed with AR-siRNA on the self-renewal of the BM-MSCs, and found that the lentiviral infection significantly enhanced the self-renewal of the BM-MSCs (Figure 8G). Finally, we tested the effects of those compounds in the BM-MSCs self-renewal with CFU-*f* assay in the presence of exogenous ligand treatment and obtained similar results (Supplemental Figure 6).

Collectively, the three current available approaches of targeting AR all resulted in the consistent conclusion that targeting AR in BM-MSCs increases their self-renewal.

Discussion

BM-MSCs transplantation has been widely applied in the clinical trials to treat diseases such as myocardial infarction, osteogenesis imperfecta, and liver cirrhosis. However, most of these clinical trials using BM-MSC transplantation to treat patients exhibit short-term improvement followed with recurring symptoms. The possible mechanism of this recurrence might be due to low numbers of BM-MSCs that are reaching to the target organs [34–37]. Meanwhile, gender differences have been shown in the function of activated BM-MSCs which are responsible for the stress challenge, such as oxidative stress [9, 10]. Therefore, our studies attempt to clarify whether the role of AR is essential in order to better utilize BM-MSCs in the clinic. The results of this study are the first demonstration showing depletion of AR enhances the self-renewal potential of BM-MSCs via elevated EGFR without influencing differentiation and apoptosis.

The female sexual hormone and its receptors, estrogen receptor α and β , are other crucial determinant mechanisms in gender dimorphism. It has been shown that estrogens promote proliferation of embryonic stem cells via promoting the MAPK cascade to affect the important cell cycle components, cyclins D1 and E [38]. The effects of estrogen on BM-MSCs have also been suggested in *in vitro* apoptosis and *in vivo* myocardial recovery. Estrogen inhibits the apoptosis of BM-MSCs through the Bcl-xL and Bcl2. Estrogen treatment improves the therapeutic effect of BM-MSCs in the myocardial recovery after ischemia [39, 40]. In the neural stem cells, estrogen plays a positive role in inducing the neuronal phenotype from embryonic stem cells and stimulating the proliferation of embryonic neural stem cells [41, 42]. However, estrogens seem to suppress the hematopoietic stem cells population and differentiation. It has been shown that male infants have a higher median CD34+ concentration in their cord blood than female infants. Also, estrogens negatively influence the production of B cells by changing the differentiation, proliferation, and survival of B cell precursors.

For the androgenic effects on the stem cell behaviors, the previous studies mainly used androgen treatments to explore the influence of male sexual hormones in stem cells. Chang et al. demonstrated that anti-androgens, such as nilutamide, could stimulate the growth of ESCs, but testosterone has no effects on the growth of ESCs [16]. For the osteoprogenitors, it has also been shown that testosterone has no effects on BM-MSC differentiation into osteoblasts [43], but AR deficiency inhibits osteogenic differentiation [44]. In addition, high doses of androgen increased the cardiomyocyte differentiation in ESCs [45]. However, AR effect has never been tested in the self-renewal potential of BM-MSCs and it should be acknowledged that the androgenic effects and the AR effects are not always the same, such as androgen and AR influence the osteogenic differentiation of BM-MSCs differentially. We are the first to identify that AR plays a suppressive role in the self-renewal of BM-MSCs with clear demonstrations that depletion of AR stimulates the self-renewal potential of BM-MSCs through elevating EGFR expression. The increased EGFR activates the signaling pathways of Akt and Erk. The inhibitor studies using PD98059 (MEK1 inhibitor) and LY294002 (inhibitor of phosphatidylinositol 3 kinase) indicated that blocking of these two signaling pathways abolishes the AR knockout effects on the increased self-renewal of BM-MSCs. Further studies using the p-EGFR inhibitor to challenge ARKO BM-MSCs exhibited that the inhibitory effects of AR on the self-renewal of BM-MSCs are through EGFR signaling. Since those inhibitors might have side effects on other pathways, we therefore directly applied the EGF to the WT BM-MSCs to see whether AR mediated BM-MSCs self-renewal is EGFR dependent. Indeed, EGF activated EGFR signaling increased the self-

renewal potential of WT BM-MSCs that have intact AR. Based on these data, it can be concluded that AR plays a suppressive role in the self-renewal of BM-MSCs by inactivating Akt and Erk signaling via down-regulating EGFR.

With our clarification of the AR role in enhancing the self-renewal of BM-MSCs, a question may arise as to whether the current available compounds can be applied to target AR and result in increased self-renewal potential of BM-MSCs. We have tested the effects of three AR targeting approaches, ASC-J9[®] (AR degradation enhancer), HF (antagonist of AR), and AR-siRNA on self-renewal of BM-MSCs. All of them showed significant enhancements in the self-renewal potentials of BM-MSCs. The chemical castration method using anti-androgen has been applied for many decades, but this method has the side-effects of restraining patient libido and fertility. On the other hand, despite many recent successful improvements, whether the delivery of siRNAs is effective without any unexpected side effects is another serious issue we currently face. However, the use of ASC-J9[®], which has been reported to degrade AR selectively in different cell types without influencing mouse fertility, and has limited side effects, could be an alternative choice. This drug has successfully completed the Phase II clinical trials (<http://www.androscience.com/artman/publish/news/press-release030609.shtml>).

In summary, we clearly demonstrated that; (i) the depletion of AR enhances the self-renewal potentials of BM-MSCs and ADSCs, but does not significantly affect differentiation and apoptosis of BM-MSCs, and (ii) we dissected the molecular mechanism by which knockout of AR enhances the self-renewal of BM-MSCs through up-regulation of EGFR. The elucidation of this study does not only indicate the suppressive role of AR in self-renewal potential of BM-MSCs but also provides evidence that degrading AR with the currently available compounds can exert the similar effects. These novel findings imply a possibility of targeting AR in BM-MSCs in clinical applications to improve the efficiency of BM-MSC transplantation in treating various diseases, such as liver cirrhosis, sepsis, autoimmune diseases, and myocardial infarction.

Materials and Methods

Cells, animals and reagents

C3H10T1/2 and D1 cells were purchased from ATCC (Manassas, VA) and the used culture conditions were used as shown in the manual. The BrdU labeling kit was purchased from ZYMED Invitrogen (Grand Island NY). All animal studies followed the “Guide for the Care and Use of Laboratory Animals” (National Institutes of Health publication). The protocols were reviewed and approved by the University Committee on Animal Resources of University of Rochester. We used Cre-Lox strategy to generate WT and ARKO mice. The floxed AR/AR mice were established in our previous publication [19]. WT and ARKO mice were established by mating floxed AR/AR female mice with Actb Cre^{+/+} mice. The floxed AR/Y-Actb Cre^{+/-} mice were used as ARKO and AR/Y-Actb Cre^{+/-} were used as WT control. Oil red O and alizarin red were purchased from Sigma-Aldrich (St. Louis, MO).

Isolation of BM-MSCs

For the isolation of mouse BM-MSCs, we followed the protocol described previously [46]. Briefly, tibias and femurs were dissected from adult mice at 8–10 weeks old. After bones were cut, the marrows were flushed out with 5 ml DMEM by using a needle and syringe, and resuspended in DMEM plus 15% FBS. After counting, about 2×10^6 mononucleated cells were plated on 25 cm² plastic flask in DMEM (Gibco), supplemented with 15% fetal bovine serum (FBS), 2 mM L-glutamine, 100 U/ml penicillin, 100 mg/ml streptomycin, and 10 mM HEPES. All of the cells were incubated at 37°C with 5% humidified CO₂. After the

first 24 hr, we removed the non-adherent cells by replacing the medium every 3 or 4 days for about 3 weeks. When the cells grow to confluence, they were harvested with 0.25% trypsin and 1 mM EDTA (Hyclone) for 5 min at 37°C, re-plated on 25 cm² plastic flask, again cultured to next confluence, and harvested.

Isolation of ADSCs

ADSCs were isolated as described in Ning *et al.* [47]. Briefly, subcutaneous adipose were removed with sterile forceps and scissors from the inguinal region of male mice and then minced to small pieces. Tissues were mixed with 3 volumes of phosphate buffer saline (PBS) and then centrifuged at 1000 rpm for 5 min. Pellets were digested with 0.075% collagenase (Sigma-Aldrich) for 1 h at 37°C with shaking. After digestion, the mixture was centrifuged at 1000 rpm for 5 min, rinsed in 10 ml PBS and centrifuged at 1000 rpm for 5 min. 10 ml DMEM with 10% FBS was added to the pellet, resuspended, and filtered through 100 µm cell strainer (BD Bioscience). Cell pellets were put into culture dish and then cultured for 3–5 days at 5% CO₂ incubator to get colonies of ADSCs.

EGFR promoter construction

EGFR promoter regions were amplified by using PCR with these primers. Forward (–2396) 5′-GGGGTACCCCAAGCTCCCCTCCCACATATGT, forward (–831) 5′-GGGGTACCCCTGGGATCTGAAGGACCCTTGA, and reverse 5′-CCGCTCGAGCGGCATCTCTGACCGGGAGAGGTT. After amplifying, we used KpnI and MluI to digest the PCR product and pGL3 vector (Promega) at 37°C overnight. We then purified the digested fragment with Qiagen Gel purification kit following the instruction manual. The purified inserter and vector were ligated together with T4 ligase at 16 °C overnight. The ligated product was transformed with DH5α, applied on the LB agar plate containing 100µg/ml ampicillin, incubated at 37°C overnight. The survival and visible clones were picked up, examined, sequenced to validate the EGFR promoter region.

CFU-f assay for Self-renewal—Primary BM-MSCs were isolated from 8 weeks old mice and then plate 2×10⁶ mononucleated cells per well onto 6-well plates. After culturing 21 days, cells were fixed with methanol and washed with ddH₂O. After washing, cells were stained with 1% methylene blue for 15 minutes and rinsed cells with ddH₂O twice. We counted colonies that have more than 20 cells as positive CFU-f.

Cell growth assay

MTT assay—MSCs were plated onto 24-well plates at the density of 5000 cells/well. At each time point indicated, MTT solution was added to cells to react for 30 minutes, medium removed, and isopropanol added to dissolve the MTT salt. The absorbance values were measured at 575 nm – 650 nm.

Ki67 staining—Stem cells were seeded on the 4-well chamber slides and cultured to confluence and then fixed with methanol. After fixation, cells were washed with PBS 3 times for 5 min each and then cells were blocked with 1% fetal bovine serum for 1 h. Cells were washed with PBS 3 times, then incubated with anti-Ki67 (NCL-Ki67p, 1:1000) in 3% BSA in PBS overnight at 4°C, and then incubated with 1:200 diluted biotinylated secondary antibody (Vector Laboratories) and ABC solution (Vector Laboratories). Cells were stained by AEC (DAKO, Carpinteria, CA), followed by Mayor's hematoxylin counterstaining.

BrdU labeling—Stem cells were seeded on the 4-well chamber slides and cultured to confluence. BrdU labeling reagent (Invitrogen) was added to the cultured cells at 1:100

dilution in the culture medium for 24 hr. After labeling, staining was performed according to the manual instruction (Invitrogen, BrdU staining kit).

Western Blot analysis assay

Antibodies used to detect the blot in this study were AR (Santa Cruz, AR C19), Erk1/2 (Cell Signaling), p-Erk1/2 (Cell Signaling), Akt (Cell Signaling), p-Akt (Cell Signaling), MEK (Cell Signaling), p-MEK (Cell Signaling), EGFR (Santa Cruz, EGFR 1005), and p-EGFR (Tyr 1173). Cell lysates were resolved with 10 % sodium dodecyl sulfate-polyacrylamide gel electrophoresis (SDS-PAGE), blotted with antibodies mentioned before, and incubated with correlated secondary antibodies conjugated with horseradish peroxidase. Proteins were visualized according to the manual instruction (Pierce ECL Western Blotting Substrate, Thermo Scientific). Tubulin served as loading control.

RNA extraction and Real Time Quantitative PCR (qRT-PCR)

Total RNAs were extracted with Trizol (Invitrogen) according to the manufacturer's instruction. Two μg mRNAs were used to reverse transcribe to cDNAs using Superscript III (Invitrogen). Quantitative qRT-PCR was performed using cDNA, specific gene primers, and SYBR green master mix (Biorad) on an iCycler iQ Multi-color real-time PCR machine (Biorad). qRT-PCR results were calculated as relative expressions to the control and normalized to the housekeeping gene, GAPDH.

Apoptosis assay (TUNEL staining)

Apoptotic death of BM-MSC was detected by using terminal deoxyribonucleotide transferase (TdT)-mediated dUTP nick-end labeling (TUNEL) detecting system as described previously [48].

Flow cytometry analysis of cell markers

BM-MSCs were detached with 0.2 % EDTA and then washed with 1% FBS in PBS (flow washing buffer). After washing, BM-MSCs were stained with CD29 PE (eBioscience), CD34 FITC (eBioscience), CD44 PE-Cy5(eBioscience), CD45 FITC (eBioscience), CD106 FITC (eBioscience), and CD117 PE (eBioscience) and washed again with 1% FBS in PBS. BM-MSCs were then resuspended in PBS and analyzed by BD Accuri® C6 Flow Cytometry. Results were further analyzed using FlowJo software according to the previous publication [49].

Adipogenesis and osteogenesis differentiations

For the adipogenesis differentiation, the isolated ADSCs and BM-MSCs were plated on 6-wells plate. After the cells reached the confluent density, the adipogenesis media (DMEM containing 10% FBS, 2 μg insulin, 10⁻⁸ M dexamethasone, and 2 μM rosiglitazone) were added to induce adipogenesis differentiation [50]. After lipid vacuole structures were observed, the Oil O red staining was used to visualize the lipid vacuoles. For the osteogenic differentiation, the confluent ADSCs and BM-MSCs were treated with osteogenic media (DMEM containing 10% FBS, 50 μg ascorbic acid, and 10mM β -glycerophosphate) to induce mineralization [51]. The mineralized osteocytes were visualized using Alizarin Red staining.

Lentivirus Infection

HEK-293T cells were used to produce lentivirus by calcium-phosphate transfection. 12 μg of lentivirus plasmid (pLVTHM-scramble, pLVTHM-AR-siRNA, pWPI, pWPI-AR), 8 μg of CMVdeltaR8.91 (contains GAG, POL) 10 μg of pMD2.G (contains VSVg) were used to produce virus in 10-cm² dish. Culture medium containing virus was collected 32 hrs after

transfection and filtrated through 0.4 μm filter to remove cell debris or cells. The collected virus were added to the target cells in the presence of polybrene (2 $\mu\text{g}/\text{ml}$) to incubate for 24 hr. Cells were refreshed with osteogenic media and cultured for another 3 days to let target protein express. Since the lentiviral vectors express green fluorescence protein, fluorescence microscopy was used to monitor the infection efficiency via checking the green fluorescence signal.

Transfection and stable clone selection

Cells were transfected with lipofectamine 2000 (Invitrogen) according the manufacturer's instructions and then desired clones were selected using appropriate antibiotics. For C3H10T1/2 cells, 600 $\mu\text{g}/\text{ml}$ G-418 and 0.5 $\mu\text{g}/\text{ml}$ puromycin were used to select stable scramble, AR-siRNA, vector, and AR clones. For ESD3, 300 $\mu\text{g}/\text{ml}$ G-418 and 0.5 $\mu\text{g}/\text{ml}$ puromycin were used to select stable clones.

GAL4-Elk1 transactivation assay

For the Elk1 transactivation assay, C3H10T1/2 cells were seeded on the 24-well plates one day before transfection [52]. pG5-luciferase, GAL4-Elk1, pCDNA3.1-flag-AR were used to identify Elk1 transactivation. pRL-TK was used as internal control.

Inhibitor studies of p-Erk1/2, p-Akt and p-EGFR

For the inhibitor study, primary BM-MSCs were isolated from either WT or ARKO mice. BM-MSCs were plated for culture with 10 μM PD98059 (Cell signaling), 10 μM Lys94002 (Cell signaling), or 0.5 μM AG1478 (Sigma), replenished every other day. After 21 days, CFU-f were visualized with 10% Giesma staining or 1% methyl blue staining.

Statistical analysis

Values were expressed as mean \pm standard deviation (S.D.). The Student's *t* test was used to calculate *P* values. *P* values were two-sided, and considered statistically significant when <0.05 .

Supplementary Material

Refer to Web version on PubMed Central for supplementary material.

Acknowledgments

We thank Karen Wolf (University of Rochester) for help in editing the manuscript. This work was supported by NIH grants (CA122840 and CA156700), and Taiwan Department of Health Clinical Trial and Research Center of Excellence (DOH99-TD-B-111-004 to China Medical University, Taiwan.)

References

1. Strauer BE, Brehm M, Zeus T, Kosterling M, Hernandez A, Sorg RV, Kogler G, Wernet P. Repair of infarcted myocardium by autologous intracoronary mononuclear bone marrow cell transplantation in humans. *Circulation*. 2002; 106:1913–1918. [PubMed: 12370212]
2. Horwitz EM, Prockop DJ, Fitzpatrick LA, Koo WW, Gordon PL, Neel M, Sussman M, Orchard P, Marx JC, Pyeritz RE, Brenner MK. Transplantability and therapeutic effects of bone marrow-derived mesenchymal cells in children with osteogenesis imperfecta. *Nat Med*. 1999; 5:309–313. [PubMed: 10086387]
3. Terai S, Ishikawa T, Omori K, Aoyama K, Marumoto Y, Urata Y, Yokoyama Y, Uchida K, Yamasaki T, Fujii Y, Okita K, Sakaida I. Improved liver function in patients with liver cirrhosis after autologous bone marrow cell infusion therapy. *Stem Cells*. 2006; 24:2292–2298. [PubMed: 16778155]

4. Horwitz EM, Gordon PL, Koo WK, Marx JC, Neel MD, McNall RY, Muul L, Hofmann T. Isolated allogeneic bone marrow-derived mesenchymal cells engraft and stimulate growth in children with osteogenesis imperfecta: Implications for cell therapy of bone. *Proc Natl Acad Sci U S A*. 2002; 99:8932–8937. [PubMed: 12084934]
5. Stamm C, Westphal B, Kleine HD, Petzsch M, Kittner C, Klinge H, Schumichen C, Nienaber CA, Freund M, Steinhoff G. Autologous bone-marrow stem-cell transplantation for myocardial regeneration. *Lancet*. 2003; 361:45–46. [PubMed: 12517467]
6. Schroder J, Kahlke V, Book M, Stuber F. Gender differences in sepsis: genetically determined? *Shock*. 2000; 14:307–310. discussion 310–303. [PubMed: 11028548]
7. Burt RK, Loh Y, Pearce W, Beohar N, Barr WG, Craig R, Wen Y, Rapp JA, Kessler J. Clinical applications of blood-derived and marrow-derived stem cells for nonmalignant diseases. *JAMA*. 2008; 299:925–936. [PubMed: 18314435]
8. Toma C, Wagner WR, Bowry S, Schwartz A, Villanueva F. Fate of culture-expanded mesenchymal stem cells in the microvasculature: in vivo observations of cell kinetics. *Circulation research*. 2009; 104:398–402. [PubMed: 19096027]
9. Crisostomo PR, Wang M, Herring CM, Morrell ED, Seshadri P, Meldrum KK, Meldrum DR. Sex dimorphisms in activated mesenchymal stem cell function. *Shock*. 2006; 26:571–574. [PubMed: 17117131]
10. Crisostomo PR, Wang M, Herring CM, Markel TA, Meldrum KK, Lillemoe KD, Meldrum DR. Gender differences in injury induced mesenchymal stem cell apoptosis and VEGF, TNF, IL-6 expression: role of the 55 kDa TNF receptor (TNFR1). *J Mol Cell Cardiol*. 2007; 42:142–149. [PubMed: 17070836]
11. Kolf CM, Cho E, Tuan RS. Mesenchymal stromal cells. *Biology of adult mesenchymal stem cells: regulation of niche, self-renewal and differentiation*. *Arthritis research & therapy*. 2007; 9:204. [PubMed: 17316462]
12. Hu C, Wu Y, Wan Y, Wang Q, Song J. Introduction of hIGF-1 gene into bone marrow stromal cells and its effects on the cell's biological behaviors. *Cell Transplant*. 2008; 17:1067–1081. [PubMed: 19177843]
13. Xie X, Cao F, Sheikh AY, Li Z, Connolly AJ, Pei X, Li RK, Robbins RC, Wu JC. Genetic modification of embryonic stem cells with VEGF enhances cell survival and improves cardiac function. *Cloning Stem Cells*. 2007; 9:549–563. [PubMed: 18154515]
14. Matsuda T, Nakamura T, Nakao K, Arai T, Katsuki M, Heike T, Yokota T. STAT3 activation is sufficient to maintain an undifferentiated state of mouse embryonic stem cells. *EMBO J*. 1999; 18:4261–4269. [PubMed: 10428964]
15. Niwa H, Burdon T, Chambers I, Smith A. Self-renewal of pluripotent embryonic stem cells is mediated via activation of STAT3. *Genes Dev*. 1998; 12:2048–2060. [PubMed: 9649508]
16. Chang CY, Hsuw YD, Huang FJ, Shyr CR, Chang SY, Huang CK, Kang HY, Huang KE. Androgenic and antiandrogenic effects and expression of androgen receptor in mouse embryonic stem cells. *Fertility and sterility*. 2006; 85(Suppl 1):1195–1203. [PubMed: 16616092]
17. Carcamo-Orive I, Tejados N, Delgado J, Gaztelumendi A, Otaegui D, Lang V, Trigueros C. ERK2 protein regulates the proliferation of human mesenchymal stem cells without affecting their mobilization and differentiation potential. *Exp Cell Res*. 2008; 314:1777–1788. [PubMed: 18378228]
18. Li J, Wang G, Wang C, Zhao Y, Zhang H, Tan Z, Song Z, Ding M, Deng H. MEK/ERK signaling contributes to the maintenance of human embryonic stem cell self-renewal. *Differentiation*. 2007; 75:299–307. [PubMed: 17286604]
19. Yeh S, Tsai MY, Xu Q, Mu XM, Lardy H, Huang KE, Lin H, Yeh SD, Altuwaijri S, Zhou X, Xing L, Boyce BF, Hung MC, Zhang S, Gan L, Chang C. Generation and characterization of androgen receptor knockout (ARKO) mice: an in vivo model for the study of androgen functions in selective tissues. *Proceedings of the National Academy of Sciences of the United States of America*. 2002; 99:13498–13503. [PubMed: 12370412]
20. Bonyadi M, Waldman SD, Liu D, Aubin JE, Grynblas MD, Stanford WL. Mesenchymal progenitor self-renewal deficiency leads to age-dependent osteoporosis in Sca-1/Ly-6A null mice. *Proc Natl Acad Sci U S A*. 2003; 100:5840–5845. [PubMed: 12732718]

21. Mitchell JB, McIntosh K, Zvonic S, Garrett S, Floyd ZE, Kloster A, Di Halvorsen Y, Storms RW, Goh B, Kilroy G, Wu X, Gimble JM. Immunophenotype of human adipose-derived cells: temporal changes in stromal-associated and stem cell-associated markers. *Stem Cells*. 2006; 24:376–385. [PubMed: 16322640]
22. Yang Z, Chang YJ, Yu IC, Yeh S, Wu CC, Miyamoto H, Merry DE, Sobue G, Chen LM, Chang SS, Chang C. ASC-J9 ameliorates spinal and bulbar muscular atrophy phenotype via degradation of androgen receptor. *Nature medicine*. 2007; 13:348–353.
23. Miyamoto H, Yang Z, Chen YT, Ishiguro H, Uemura H, Kubota Y, Nagashima Y, Chang YJ, Hu YC, Tsai MY, Yeh S, Messing EM, Chang C. Promotion of bladder cancer development and progression by androgen receptor signals. *J Natl Cancer Inst*. 2007; 99:558–568. [PubMed: 17406000]
24. Ma WL, Hsu CL, Wu MH, Wu CT, Wu CC, Lai JJ, Jou YS, Chen CW, Yeh S, Chang C. Androgen receptor is a new potential therapeutic target for the treatment of hepatocellular carcinoma. *Gastroenterology*. 2008; 135:947–955. 955 e941–945. [PubMed: 18639551]
25. Chuang KH, Altuwajri S, Li G, Lai JJ, Chu CY, Lai KP, Lin HY, Hsu JW, Keng P, Wu MC, Chang C. Neutropenia with impaired host defense against microbial infection in mice lacking androgen receptor. *J Exp Med*. 2009; 206:1181–1199. [PubMed: 19414555]
26. Miyahara Y, Nagaya N, Kataoka M, Yanagawa B, Tanaka K, Hao H, Ishino K, Ishida H, Shimizu T, Kangawa K, Sano S, Okano T, Kitamura S, Mori H. Monolayered mesenchymal stem cells repair scarred myocardium after myocardial infarction. *Nature medicine*. 2006; 12:459–465.
27. Nishino J, Kim I, Chada K, Morrison SJ. Hmga2 promotes neural stem cell self-renewal in young but not old mice by reducing p16Ink4a and p19Arf Expression. *Cell*. 2008; 135:227–239. [PubMed: 18957199]
28. Oguro H, Iwama A, Morita Y, Kamijo T, van Lohuizen M, Nakauchi H. Differential impact of Ink4a and Arf on hematopoietic stem cells and their bone marrow microenvironment in Bmi1-deficient mice. *J Exp Med*. 2006; 203:2247–2253. [PubMed: 16954369]
29. Bendall SC, Stewart MH, Menendez P, George D, Vijayaragavan K, Werbowetski-Ogilvie T, Ramos-Mejia V, Rouleau A, Yang J, Bosse M, Lajoie G, Bhatia M. IGF and FGF cooperatively establish the regulatory stem cell niche of pluripotent human cells in vitro. *Nature*. 2007; 448:1015–1021. [PubMed: 17625568]
30. Bonaccorsi L, Muratori M, Carloni V, Marchiani S, Formigli L, Forti G, Baldi E. The androgen receptor associates with the epidermal growth factor receptor in androgen-sensitive prostate cancer cells. *Steroids*. 2004; 69:549–552. [PubMed: 15288768]
31. Bonaccorsi L, Carloni V, Muratori M, Formigli L, Zecchi S, Forti G, Baldi E. EGF receptor (EGFR) signaling promoting invasion is disrupted in androgen-sensitive prostate cancer cells by an interaction between EGFR and androgen receptor (AR). *International journal of cancer Journal international du cancer*. 2004; 112:78–86. [PubMed: 15305378]
32. Yu S, Yeh CR, Niu Y, Chang HC, Tsai YC, Moses HL, Shyr CR, Chang C, Yeh S. Altered prostate epithelial development in mice lacking the androgen receptor in stromal fibroblasts. *The Prostate*. 2012; 72:437–449. [PubMed: 21739465]
33. Lai KP, Yamashita S, Vitkus S, Shyr CR, Yeh S, Chang C. Suppressed prostate epithelial development with impaired branching morphogenesis in mice lacking stromal fibromuscular androgen receptor. *Mol Endocrinol*. 2012; 26:52–66. [PubMed: 22135068]
34. Liu PY, Death AK, Handelsman DJ. Androgens and cardiovascular disease. *Endocr Rev*. 2003; 24:313–340. [PubMed: 12788802]
35. Kaushik M, Sontineni SP, Hunter C. Cardiovascular disease and androgens: A review. *Int J Cardiol*. 2010; 142:8–14. [PubMed: 19923015]
36. Yeap BB. Androgens and cardiovascular disease. *Curr Opin Endocrinol Diabetes Obes*. 2010; 17:269–276. [PubMed: 20186051]
37. Eugene D, Djemli A, Van Vliet G. Sexual dimorphism of thyroid function in newborns with congenital hypothyroidism. *J Clin Endocrinol Metab*. 2005; 90:2696–2700. [PubMed: 15728201]
38. Han HJ, Heo JS, Lee YJ. Estradiol-17beta stimulates proliferation of mouse embryonic stem cells: involvement of MAPKs and CDKs as well as protooncogenes. *American journal of physiology Cell physiology*. 2006; 290:C1067–1075. [PubMed: 16291822]

39. Ayaloglu-Butun F, Terzioglu-Kara E, Tokcaer-Keskin Z, Akcali KC. The effect of estrogen on bone marrow-derived rat mesenchymal stem cell maintenance: inhibiting apoptosis through the expression of Bcl-xL and Bcl-2. *Stem cell reviews*. 2012; 8:393–401. [PubMed: 21710144]
40. Erwin GS, Crisostomo PR, Wang Y, Wang M, Markel TA, Guzman M, Sando IC, Sharma R, Meldrum DR. Estradiol-treated mesenchymal stem cells improve myocardial recovery after ischemia. *The Journal of surgical research*. 2009; 152:319–324. [PubMed: 18511080]
41. Brannvall K, Korhonen L, Lindholm D. Estrogen-receptor-dependent regulation of neural stem cell proliferation and differentiation. *Molecular and cellular neurosciences*. 2002; 21:512–520. [PubMed: 12498791]
42. Murashov AK, Pak ES, Hendricks WA, Tatko LM. 17beta-Estradiol enhances neuronal differentiation of mouse embryonic stem cells. *FEBS letters*. 2004; 569:165–168. [PubMed: 15225627]
43. Leskela HV, Olkku A, Lehtonen S, Mahonen A, Koivunen J, Turpeinen M, Uusitalo J, Pelkonen O, Kangas L, Selander K, Lehenkari P. Estrogen receptor alpha genotype confers interindividual variability of response to estrogen and testosterone in mesenchymal-stem-cell-derived osteoblasts. *Bone*. 2006; 39:1026–1034. [PubMed: 16782420]
44. Tsai MY, Shyr CR, Kang HY, Chang YC, Weng PL, Wang SY, Huang KE, Chang C. The reduced trabecular bone mass of adult ARKO male mice results from the decreased osteogenic differentiation of bone marrow stroma cells. *Biochemical and biophysical research communications*. 2011; 411:477–482. [PubMed: 21723262]
45. Goldman-Johnson DR, de Kretser DM, Morrison JR. Evidence that androgens regulate early developmental events, prior to sexual differentiation. *Endocrinology*. 2008; 149:5–14. [PubMed: 17916626]
46. Peister A, Mellad JA, Larson BL, Hall BM, Gibson LF, Prockop DJ. Adult stem cells from bone marrow (MSCs) isolated from different strains of inbred mice vary in surface epitopes, rates of proliferation, and differentiation potential. *Blood*. 2004; 103:1662–1668. [PubMed: 14592819]
47. Ning H, Lin G, Lue TF, Lin CS. Neuron-like differentiation of adipose tissue-derived stromal cells and vascular smooth muscle cells. *Differentiation*. 2006; 74:510–518. [PubMed: 17177848]
48. Niu Y, Altuwaijri S, Yeh S, Lai KP, Yu S, Chuang KH, Huang SP, Lardy H, Chang C. Targeting the stromal androgen receptor in primary prostate tumors at earlier stages. *Proc Natl Acad Sci U S A*. 2008; 105:12188–12193. [PubMed: 18723670]
49. Lai JJ, Lai KP, Chuang KH, Chang P, Yu IC, Lin WJ, Chang C. Monocyte/macrophage androgen receptor suppresses cutaneous wound healing in mice by enhancing local TNF-alpha expression. *The Journal of clinical investigation*. 2009; 119:3739–3751. [PubMed: 19907077]
50. Lin HY, Xu Q, Yeh S, Wang RS, Sparks JD, Chang C. Insulin and leptin resistance with hyperleptinemia in mice lacking androgen receptor. *Diabetes*. 2005; 54:1717–1725. [PubMed: 15919793]
51. Kang HY, Shyr CR, Huang CK, Tsai MY, Orimo H, Lin PC, Chang C, Huang KE. Altered TNSALP expression and phosphate regulation contribute to reduced mineralization in mice lacking androgen receptor. *Molecular and cellular biology*. 2008; 28:7354–7367. [PubMed: 18838539]
52. Yeh S, Hu YC, Wang PH, Xie C, Xu Q, Tsai MY, Dong Z, Wang RS, Lee TH, Chang C. Abnormal mammary gland development and growth retardation in female mice and MCF7 breast cancer cells lacking androgen receptor. *J Exp Med*. 2003; 198:1899–1908. [PubMed: 14676301]

Highlights

- Knockout of AR enhances self-renewal potential in MSCs through EGFR/ERK/AKT.
- AR inhibits self-renewal potentials of MSCs.
- Targeting AR in MSCs might lead to better transplantation therapeutic efficacy.

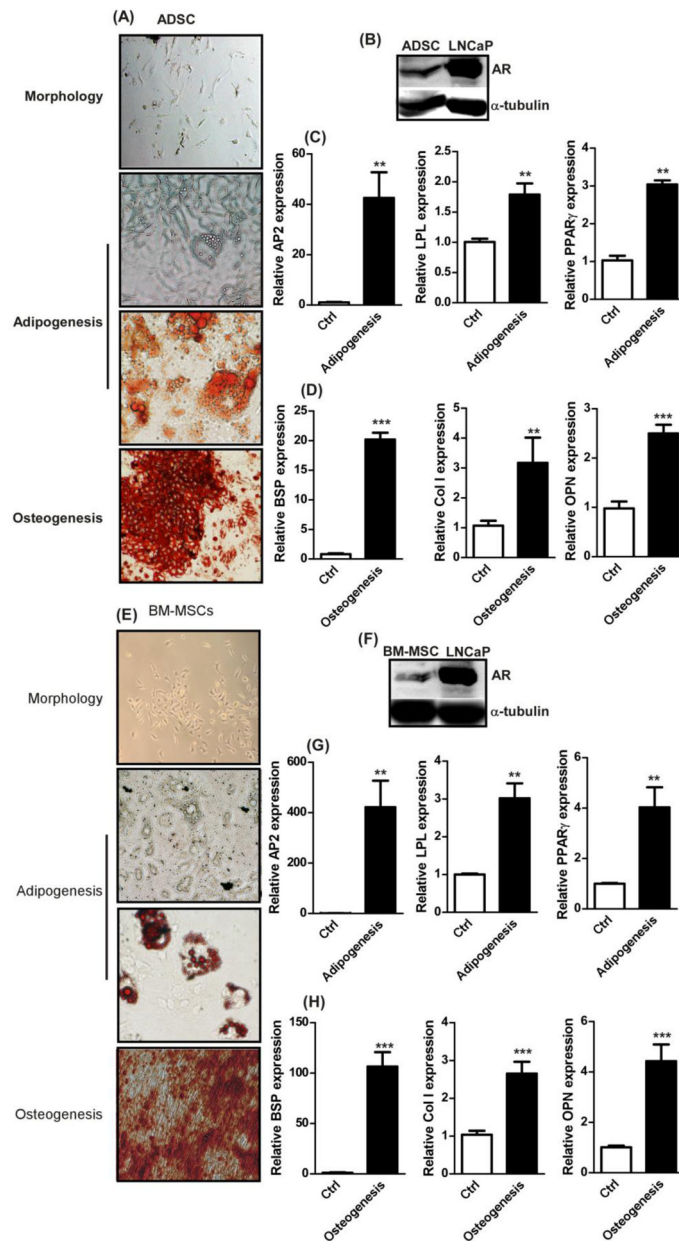


Figure 1. Identification of stem cell characteristics

(A) Representative images of morphology, adipogenesis, and osteogenesis of isolated primary ADSCs. Adipogenesis was confirmed with oil droplets, vacuole like structure, and oil red O staining (red color). Osteogenesis was confirmed with Alizarin red staining (red color). (B) Western blot results of AR and α -Tubulin in ADSCs and LNCaP, positive control for AR. qRT-PCR was used to quantify the marker expressions of (C) AP2, LPL, and PPAR γ for adipogenesis and (D) BSP, Col1, and OPN for osteogenesis in ADSC. Ctrl is vehicle control without differentiation induction. (E) Representative images of morphology, adipogenesis, and osteogenesis for BM-MSCs. (F) Western blot results of AR and α -Tubulin in BM-MSCs and LNCaP. (G) Adipogenesis and (H) osteogenesis marker expressions in BM-MSCs. $n = 5$, *, p -value < 0.05 , **, p -value < 0.005 when compared with controls. Student t test was used to perform statistical analysis.

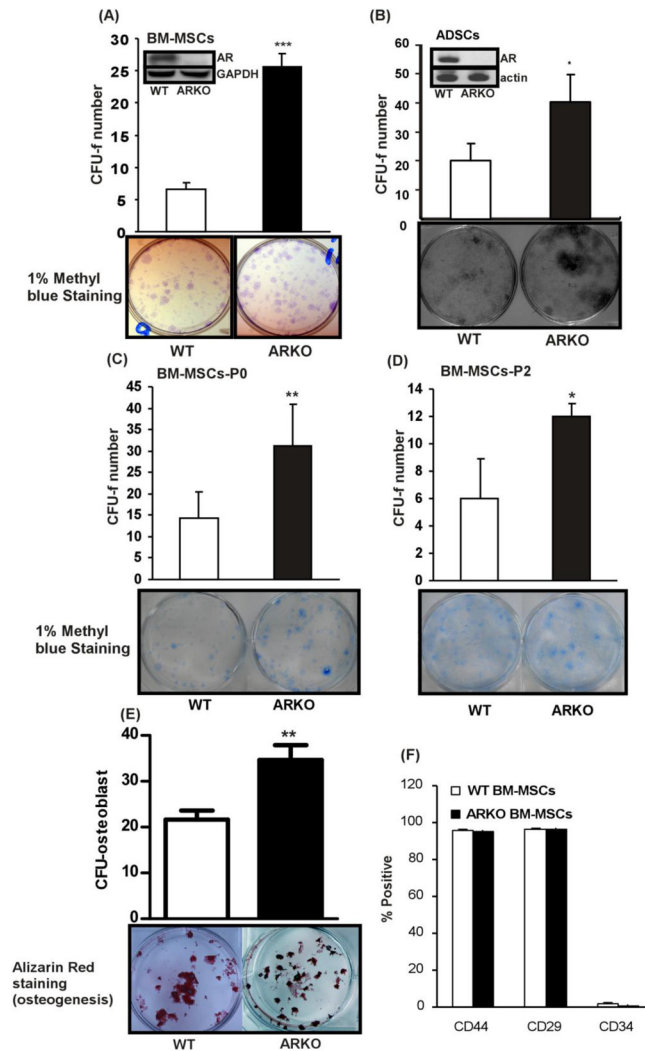


Figure 2. AR suppresses self-renewal of BM-MSCs and ADSCs

(A) CFU-f tests representing self-renewal abilities of BM-MSCs and ADSCs were performed with BM-MSCs of WT and ARKO mice. BM-MSCs isolated from 8 weeks old WT and ARKO mice were seeded onto 6-well plates and the colonies formed were stained with 1% methyl blue. Colonies with more than 20 cells were counted as positive, ($n = 9$). (B) ADSCs isolated from 8 weeks old WT and ARKO mice were seeded onto the 6-well culture plates and CFU-f assay was performed (C-D) CFU-f tests were performed with (C) BM-MSCs of passage 0 and (D) BM-MSCs of passage 2. (E) Alizarin red staining was performed to determine differentiation of BM-MSCs into osteoblasts. Presented CFU-O numbers were reflective of colony forming ability. (F) Flow cytometry results in CD44, CD29, and CD34 were shown in WT and ARKO BM-MSCs. **, p -value < 0.005 when comparing with control, $n = 5$. *, p -value < 0.05, **, p -value < 0.005 when compared with controls.

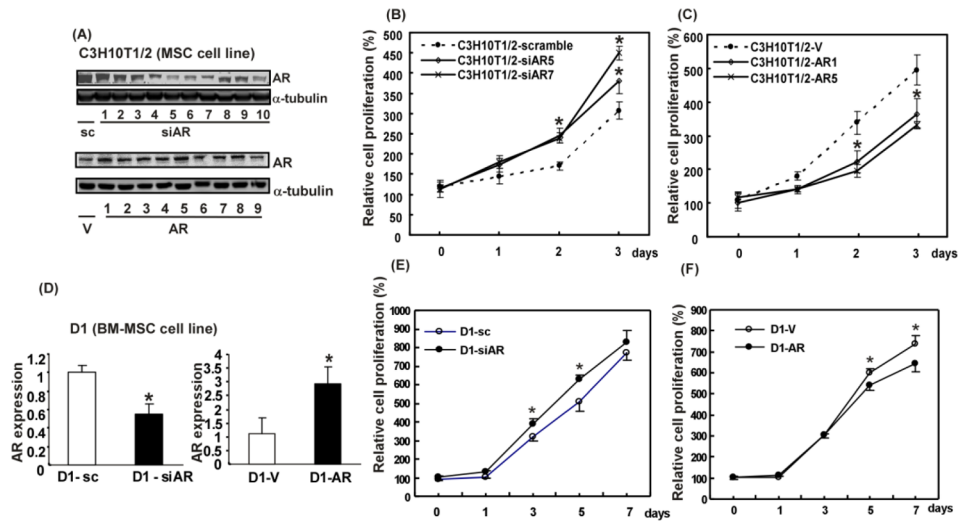


Figure 3. AR is critical in growth of stem cells

(A) Western blot analysis of AR expressions in AR overexpressing and knocked down C3H10T1/2 clone cells. α -tubulin served as internal control. Numbers represent different clones. MTT assays were performed in C3H10T1/2 cell lines which were manipulated (B) either with AR knocked down (siAR5, siAR7) and scramble control or (C) with AR overexpression (AR1, AR5) and vector control. Cell growth at days 0, 1, 2, and 3 was analyzed. (D) qRT-PCR analysis result of AR mRNA expressions in virus infected D1 cells. (E, F), MTT assays were also performed with D1 cell line. (E), with AR knocked down clone and scramble control cells, (F), with AR overexpressing clone and vector control cells. Cell growth at days 0, 1, 2, and 3 was analyzed. *, p -value < 0.05, when compared to the control.

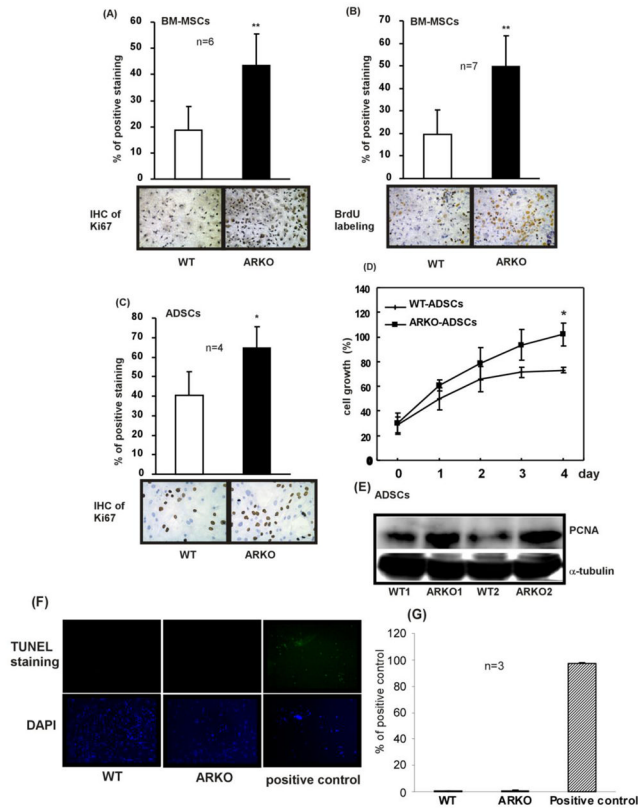


Figure 4. Depletion of AR in BM-MSCs and ADSCs stimulates their proliferation

(A) IHC staining result of Ki67. BM-MSCs isolated from 8 weeks old WT and ARKO mice were seeded on culture plates. Percentage of positive staining was expressed as positive Ki67 signals/total nuclear signals, $n = 6$. (B) BrdU labeling experiment result. Percentage of positive staining was calculated as positive BrdU signals/total nuclear signals, $n = 7$. (C) IHC staining result of Ki67 in ADSCs that were isolated from 8 weeks old WT and ARKO mice, $n = 4$. (D) MTT assay result of ADSCs of WT and ARKO mice. Percentage of growth was normalized to the highest value (set as 100%). (E) Western blot analysis showing expression of PCNA in ADSCs obtained from the WT (WT1 and WT2) and the ARKO (ARKO1 and ARKO2) mice. α -Tubulin was used as control. (F) TUNEL staining was performed according the manufacturer's instruction to examine apoptotic death of BM-MSCs of WT and ARKO mice. Positive control provided in the TUNEL assay kit was applied. Green fluorescence signal represents the positive apoptosis signal. (G) Quantitation of TUNEL staining results. *, p -value < 0.05, **, p -value < 0.01, when compared to controls.

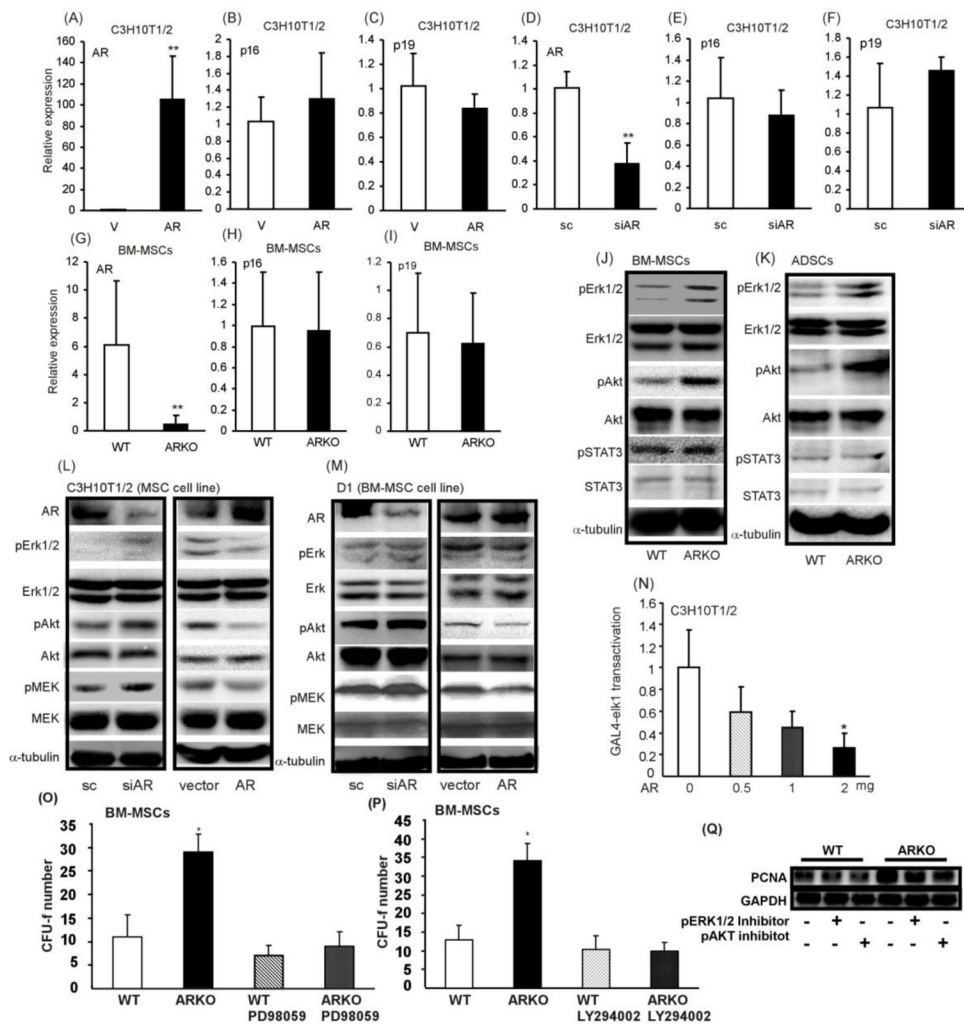


Figure 5. Erk1/2 and Akt signals are critical in AR knockout enhanced self-renewal of BM-MSCs

(A) – (I), qPCR analysis results of AR, p16 and p19 in C3H10T1/2 and primary BM-MSCs after manipulation of AR either with overexpression or knockdown. (A)–(F) with C3H10T1/2 cell line and (G)–(I) with primary BM-MSCs. BM-MSCs were isolated from 8 weeks old WT and ARKO mice. (J, K) Western blot analysis results of STAT3, p-STAT3, Erk1/2, p-Erk1/2, Akt, and p-Akt in primary (J) BM-MSCs and (K) ADSCs. (L, M), Western blot analysis results of p-Erk1/2, Erk1/2, p-Akt, Akt, p-MEK, and MEK in (L) C3H10T1/2 and (M) D1 cells after transfecting with either AR-siRNA (with scramble control) or AR (with vector control). (N) Elk transactivation assay was performed by co-transfection of AR, GAL4-Elk, and pG5-luciferase plasmids into C3H10T1/2 cells. BM-MSCs were isolated from WT and ARKO mice, seeded on 6-well plates at density of 2×10^6 /well, treated with (O) $10 \mu\text{M}$ PD98059 and (P) $10 \mu\text{M}$ LY294002, and CFU-f numbers were examined. PD98059 and LY294002 were administered to the culture media every 2 days until completion of experiments. *, p-value < 0.05, **, p-value < 0.01, when compared to the control.

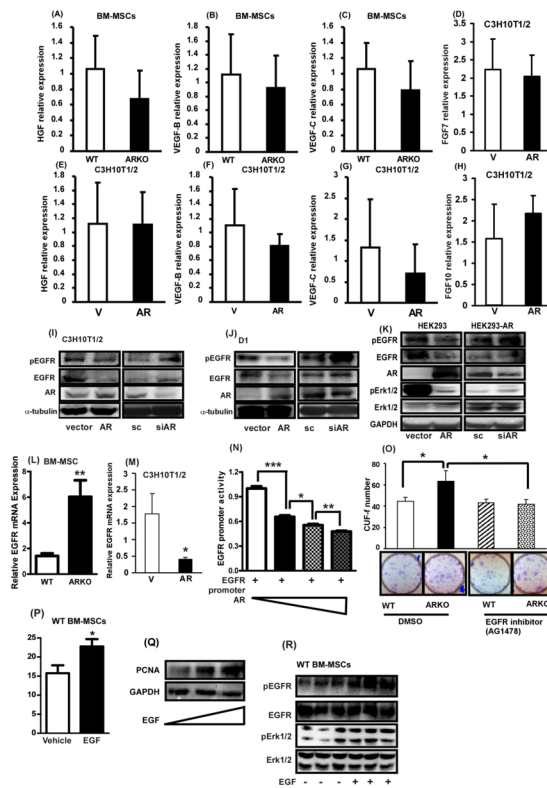


Figure 6. The activation of Akt and Erk signaling in AR knocked out BM-MSCs is through EGF/EGFR

(A)–(H) qPCR analysis results of HGF, VEGF-B, VEGF-C, KGF, and FGF-10 in primary BM-MSCs and C3H10T1/2 cell line. BM-MSCs were isolated from WT and ARKO mice at ages of 8–12 weeks. (A–C) are the results obtained with primary BM-MSCs isolated from WT and ARKO mice and (D–H) represent the results with C3H10T1/2 cell line after manipulation of AR expression. (I–K) Western blot results in expression levels of EGFR, and p-EGFR in (I) C3H10T1/2, (J) D1, (K) HEK293 cell lines after manipulation of AR expressions. (L, M) qPCR analysis results of EGFR in (L) primary BM-MSCs of WT and ARKO mice and (M) C3H10T1/2 cell line after AR overexpression. (N) EGFR promoter assay was performed in HEK-293T cells. From lanes 1 to 4, AR was increasingly added to the experimental set as drawn in the image. (O) CFU-f test result of BM-MSCs of WT and ARKO mice after treatment with EGFR inhibitor (AG1478, 0.5 μ M). (P) 20 ng/ml EGF was used to treat WT BM-MSCs to see EGF effect on the CFU-f and (Q) pEGFR, EGFR, pErk1/2, and pErk1/2 were measured using western blot. *, p -value < 0.05, **, p -value < 0.01, when compared with control.

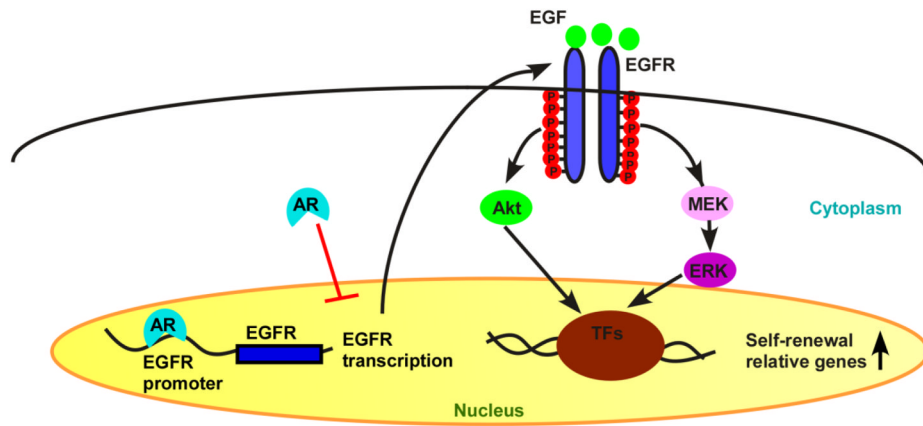


Figure 7. Illustration of AR mediated EGFR signaling in BM-MSC self-renewal
Transcriptional factors (TFs)

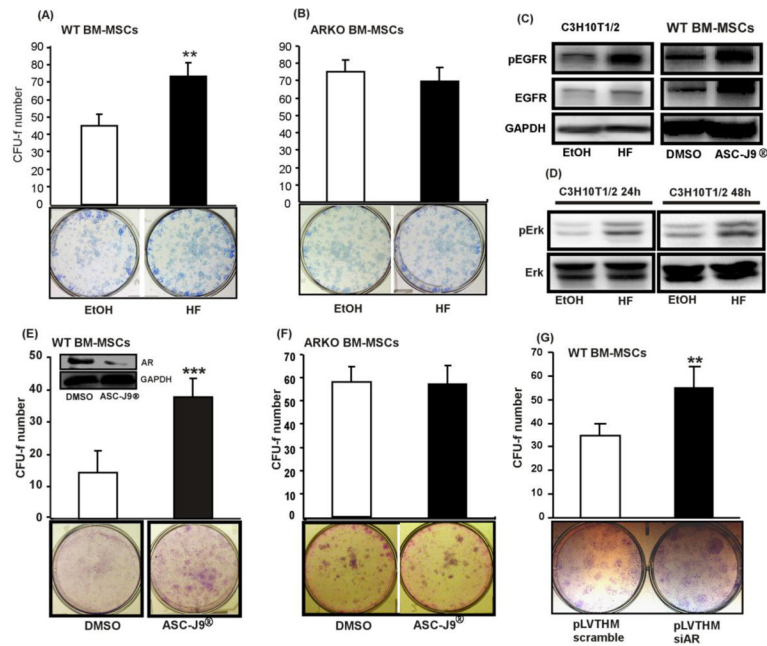


Figure 8. Blocking the androgen/AR signaling increased the self-renewal of BM-MSCs in WT mice, but not in ARKO mice

CFU-f test results of primary BM-MSCs of (A) WT and (B) ARKO mice in the presence of EtOH (vehicle) or 1 μ M HF. (C) pEGFR and EGFR expressions in C3H10T1/2 upon HF treatment (left panel) and primary WT BM-MSCs treated with ASC-J9® (right panel). (D) Western blot analysis results of pErk1/2 and Erk1/2 levels in C3H10T1/2 cells that were treated with vehicle or 1 μ M HF. (E, F) CFU-f test results of BM-MSCs that were treated with DMSO (vehicle) or 5 μ M ASC-J9®. (G) CFU-f test results of WT BM-MSCs that were infected with lentivirus packed with either scramble or AR-siRNA, **, p -value < 0.01, ***, p -value < 0.001, when compared to the control.